Topographically selective deposition

Ahmad Chaker, Christophe Vallée, Vincent Pesce, Samia Belahcen, Rémi Vallat, Rémy Gassilloud, Nicolas Possémé, Marceline Bonvalot, A. Bsiesy

Applied Physics Letters ARTICLE scitation.org/journal/apl

Topographically selective deposition

Cite as: Appl. Phys. Lett. **114**, 043101 (2019); doi: 10.1063/1.5065801
Submitted: 11 October 2018 · Accepted: 12 January 2019 · Published Online: 28 January 2019

A. Chaker,[1] C. Vallee,[1] V. Pesce,[1,2] S. Belahcen,[1] R. Vallat,[1] R. Gassilloud,[2] N. Posseme,[2] M. Bonvalot,[1] and A. Bsiesy[1,a)]

AFFILIATIONS

[1] University Grenoble Alpes, CNRS, LTM, F-38000 Grenoble, France
[2] CEA, LETI, Minatec Campus, F-38054 Grenoble, France

[a)] **Author to whom correspondence should be addressed:** Ahmad.bsiesy@univ-grenoble-alpes.fr

ABSTRACT

In this paper, we present a topographically Selective Deposition process which allows the vertical only coating of three-dimensional (3D) nano-structures. This process is based on the alternate use of plasma enhanced atomic layer deposition (PEALD) and sputtering carried out in a PEALD reactor equipped with a radio-frequency substrate biasing kit. A so-called super-cycle has been conceived, which consists of 100 standard deposition cycles followed by an anisotropic argon sputtering induced by the application of a 13.56 MHz biasing waveform to the substrate holder in the PEALD chamber. This sputtering step removes the deposited material on horizontal surfaces only, and the sequential deposition/etch process allows effective deposition on vertical surfaces only. Thus, it opens up a route for topographically selective deposition, which can be of interest for the fabrication of 3D vertical Metal-Insulator-Metal devices.

The ongoing pace of size reduction along with the introduction of materials in recent microelectronic devices truly challenges lithography techniques beyond the 5 nm node.[1] The traditional top-down approach becomes more and more time consuming and expensive, and most importantly, pattern alignment tolerances become very hard to maintain at the nm scale. Area selective deposition (ASD) has recently been developed as a time- and cost-effective solution based on a bottom-up approach for accurate self-aligned patterning at the nm scale without any lithography step.[2–4] Thus, the ASD process prevents any misalignment errors and should help strongly reduce patterning costs due to multiple patterning steps for chip production below the 5 nm node.[1,3] Atomic layer deposition (ALD) is the suitable deposition technique for area selective deposition, and much progress on ASD has been made in the last few years based on monitoring self-limited surface reactions by surface passivation, activation, or inhibition.[5–24]

Until very recently, plasma-enhanced ALD tools were designed with the idea that any ion bombardment on the substrate surface should be avoided in order to minimize any plasma-induced defects. Thus, ALD plasma assistance relies on radical species only, independent of the plasma discharge type, whether capacitive or inductive.[25] However, in PECVD processes, ion bombardment is known to positively impact the growth rate and microstructure and physical properties of the obtained thin films.[26] Thus, it is potentially of interest to take advantage of the ion bombardment energy extracted from the plasma in plasma enhanced (PE)-ALD processes. For this purpose, a specific PEALD chamber design has been lately developed by Oxford Instruments, which is equipped with a waveform bias kit system at the backside of the substrate. With this 13.56 MHz radio-frequency (RF) substrate biasing, it becomes possible to modulate the energy of ions extracted from the plasma source and in turn to tune the growth per cycle (GPC) and thin film properties. For instance, Kessels *et al.* have reported a GPC increase during the deposition of HfO_2, TiO_2, and HfN thin films, and a decrease in the case of TiN and SiO_2 thin films.[26–28] In the same vein, Karwal *et al.* have observed a steady decrease in the electrical resistivity of HfN_x films by two orders of magnitude when the time-averaged substrate potential is increased up to −130 V.[29]

The aim of the present work is to develop a topographically selective deposition process in a 3D patterned substrate, by intercalating a sputtering step within a standard PEALD deposition process. The benefits of etching combined with PEALD processes for ASD have been discussed in a previous paper on ASD of oxides on metallic surfaces, on both 2D[24] and 3D surfaces.[30] Here, we propose to develop this process for a topographically ASD on vertical features. Recently, ASD on vertical nano-pillars using SAM molecules has been achieved by Dong *et al.*[31] with a

process requiring several deposition steps and a final gold removal step on non-coated surfaces: at first, gold is deposited on the top and bottom horizontal surfaces of the pillars by an anisotropic physical vapor deposition process. SAM molecules are then selectively grafted on the gold coated area to prevent any ZnO deposition on horizontal surfaces in the subsequent ALD step. Thus, only vertical surfaces of the standing nano-pillars are coated.[9] Recently, Kim *et al.* also realized the topographically selective growth of Pt thin films along vertical sidewalls using an initial CF_x^+ plasma-based ion implantation treatment.[32]

The basic principle of the process that we have developed is similar to the high-density plasma chemical vapor deposition (HDP-CVD) process for gap-filling of sub-half-micron wide gaps to avoid void formation in semiconductor manufacturing. It relies on a simultaneous deposition and etching process whereby loosely deposited materials that tend to accumulate on trench corners are preferentially sputtered off *in situ* by Ar^+ ions in order to leave the top of the trench opened to radicals and reactive ions for filling.[33] The topographically ASD process that we have developed consists of two steps, as illustrated in Fig. 1. First, a thin isotropic layer is deposited in a standard PEALD step. Second, its anisotropic etching is performed by argon sputtering leading to a selective deposition on sidewalls only. The key-benefit of this ASD approach is the fact that it is very easy to implement, each step being carried out within the same experimental tool, and no subsequent gold or SAM etching step being required.

This selective deposition along vertical sidewalls can be applied for the fabrication of coaxial 3D metal-insulator-metal (MIM) capacitors with increased capacitance density, where all layered materials are deposited within the very same PEALD biased substrate chamber. Such a 3D coaxial MIM architecture is an interesting candidate for future circuits and systems, as described in Ref. 34.

However, this approach can be limited by large recombination rates of plasma radical species during PEALD deposition. Schindler *et al.* have observed poor step coverage during the deposition of TiO_2 by PEALD in structures with an aspect ratio (AR) of 1:30.[35] Further studies carried out in our laboratory (to be published) have shown that spacers with a critical dimension (CD) of 20 nm can be defined with this process.

The proof of concept of our ASD process has been carried out with Ta_2O_5 deposited on a silicon substrate. No pre-cleaning of the silicon substrate has been carried out before deposition. The Ta_2O_5 thin film is deposited by PEALD in a FlexAL reactor from Oxford Instruments using a tertbutylimido-tris-dimethylamino tantalum (TBTDMT) precursor and O_2 plasma as an oxidant, with a substrate temperature of 250 °C. The TBTDMT is heated at 60 °C and bubbled by a 100 sccm of argon flow for 1.5 s in the deposition chamber. The inductive plasma is ignited by application of a 3 s, 300 W RF power supply to the inductively coupled plasma (ICP) coil. A 200 sccm argon flow of 2 s and 3 s is used for the purge step of the precursor and of the plasma gas, respectively. Under such experimental conditions, the GPC of Ta_2O_5 on the silicon substrate is estimated at 0.1 nm/cycle.

The atomic layer etching (ALE) bias kit system implemented in the FlexAL PEALD chamber allows the accurate tuning of the ion energy during the plasma step. The backside additional RF power induces a negative dc self-bias voltage V_{dc} to the substrate, which under our experimental conditions leads to an ion energy proportional to the difference between the plasma potential V_p and V_{dc}. The substrate RF power can be tuned between 1 W and 50 W, leading to dc self-bias absolute values of a few tens of volts up to 300 V, which in turn allow accurate monitoring of ion energy values. The Ta_2O_5 thin film growth is monitored *in situ* using a Film sense FS-1 Multi-Wavelength ellipsometer, for an excellent precision of film thickness measurements during the precursor pulse and the argon purge. Patterned Si substrates are realized in a dedicated deep reactive ion etching (DRIE) equipment following a Bosch process: trenches and holes with aspect ratios (ARs) of 7 and 5, respectively, have been achieved by alternating Si etching steps by sulfur hexafluoride (SF_6) and surface passivation treatment by Octafluorocyclobutane (C_4F_8).

Figure 2 shows the *in situ* variation of the Ta_2O_5 film thickness under growth, as measured by ellipsometry, during a standard PEALD process, without ion bombardment energy. Twenty periodic patterns corresponding to 20 PEALD cycles are observed, leading to a nearly steady growth rate.

The thickness variation during only one PEALD cycle is zoomed in Fig. 3. The overall duration of the cycle is 11.5 s and five steps can be clearly identified, as described below. In the first step, the TBTDMT precursor is injected into the PEALD chamber. The metallic precursor chemisorbs on the substrate surface, with its organic ligands leading to the strong thickness increase. The second step is the precursor purge under an argon gas flow, whereby no deposition or surface modification is detected. The third step is a plasma stabilization step required to stabilize the O_2 pressure within the reactor chamber. According to the *in situ* thickness measurements, precursor molecules adsorbed at the substrate surface do not react with O_2 gas, since no thickness variation is evidenced. In step 4, chemically active oxygen species from the O_2 plasma eliminate ligands from adsorbed metallic precursors. This mechanism leads to a decrease in the thickness induced by the evacuation of organic ligands. In the final chemically inactive argon purge step, the

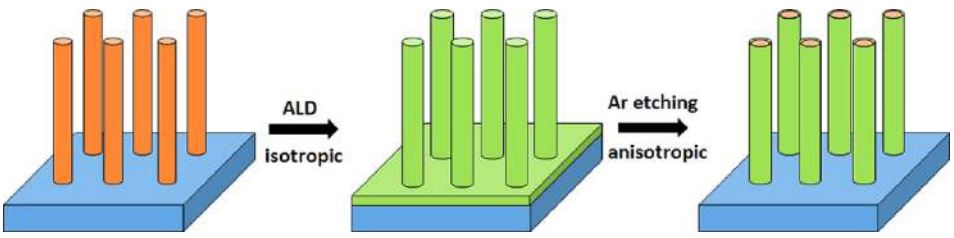

FIG. 1. Schematic diagram of topographic selectivity after ALD isotropic deposition and anisotropic argon etching.

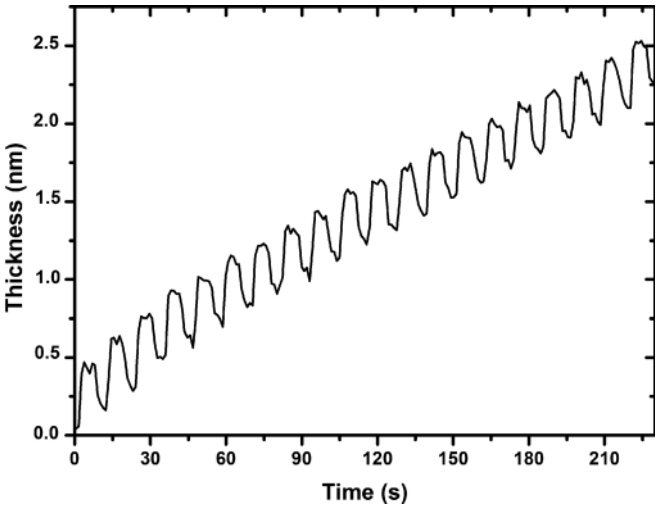

FIG. 2. *In situ* ellipsometric measurements of the Ta_2O_5 film thickness during 20 PEALD cycles.

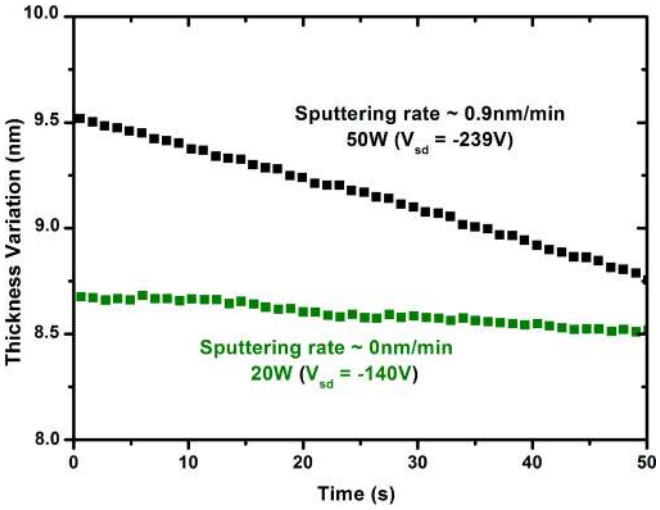

FIG. 4. Ta_2O_5 thickness variation during the argon plasma sputtering step, at two substrate bias values.

thickness shows a plateau, as expected. The overall thickness variation from the beginning to the end of one PEALD cycle thus corresponds to the GPC and is estimated at 0.1 nm/cycle.

The behavior of the as-deposited Ta_2O_5 material in pure argon plasma has been studied as a function of the ion bombardment energy. Figure 4 shows the obtained results at two substrate biasing voltage values, respectively, −140 V and −239 V. It can be seen that the Ta_2O_5 thickness does not vary significantly (around 1%) for a substrate bias of −140 V, whereas it decreases by nearly 10% for a substrate bias of −239 V. These variations correspond to a sputtering rate close to 0 nm/min at a dc self-bias of −140 V, whereas it is close to 0.9 nm/min at a dc self-bias of −239 V. These results show that a fine control of the Ar^+ plasma ion energy through substrate biasing allows in turn etching of Ta_2O_5.

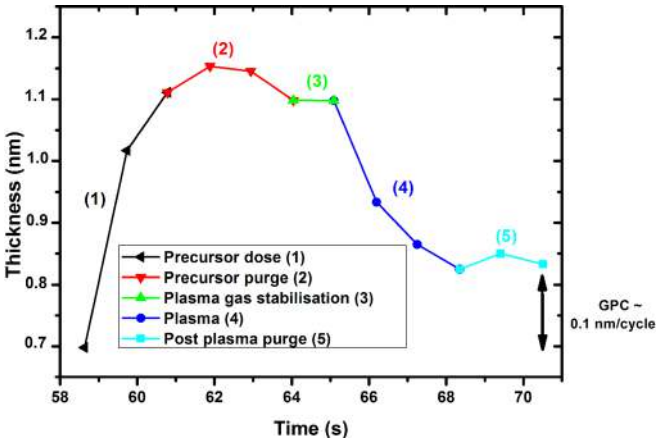

FIG. 3. Thickness variation during one PEALD cycle: 1: precursor dose (pressure 80 mTorr), 2: precursor purge, 3: plasma gas stabilization, 4: O_2 plasma step (pressure 15 mTorr), and 5: post plasma purge.

The concept of the ASD process that we have developed relies on the vertical geometry of the electric field induced by the back side substrate bias in the FlexAL tool and on the fact that only surfaces exposed to the Ar^+ plasma ion flux are preferentially etched away. We thus expect that the introduction of an Ar^+ plasma etching step within a standard PEALD deposition cycle potentially leads to a selective Ta_2O_5 removal on horizontal surfaces, without affecting Ta_2O_5 coated vertical flanks. We have carefully optimized this ASD process by defining a super cycle, as indicated in Fig. 5.

100 standard PEALD cycles lead to a conformal 10 nm thick Ta_2O_5 layer, so a 12 min Ar^+ sputtering step under a −239 V bias is required in order to etch it away. However, an additional 4 min over-etching step is added to this to ensure full etching of horizontal surfaces within the depth of the 3D patterned substrate. The so-called super-cycle has been repeated seven times to lead to a 70 nm thick anisotropic layer of Ta_2O_5.

Figure 6 shows the Ta_2O_5 thickness variation as measured by *in situ* ellipsometry during the seven super cycles of the ASD process on a non-patterned Si substrate. It can be seen that during the first super-cycle, the Ta_2O_5 deposited layer is 10 nm

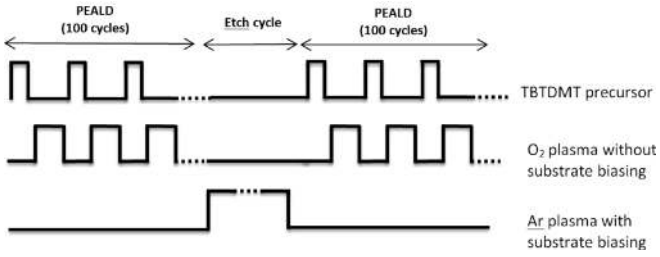

FIG. 5. Optimized process of the area selective deposition: a super-cycle corresponds to 100 PEALD cycles followed by an argon plasma etch cycle with substrate bias.

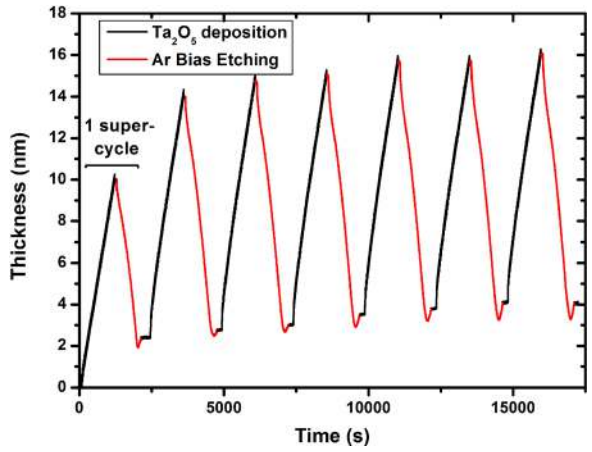

FIG. 6. *In situ* monitoring of the ASD process: Ta_2O_5 thickness variation during seven super-cycles, as a function of time.

thick after the 100 PEALD cycles. However, its measured thickness after the subsequent Ar^+ plasma sputtering step does not drop back to zero nm as expected, but instead it reaches a steady value of 2 nm, even under a longer exposure to Ar^+ ion bombardment. This 2 nm value corresponds to a thin SiO_2 layer growth at the interface between Si and Ta_2O_5 in the standard PEALD process. Under our experimental conditions, the oxidized surface of the silicon substrate is not sputtered away by the Ar^+ ion bombardment. The ellipsometry measurement indicates an oxidized thickness of the order of 2 nm (corresponding to the lowest point of the ellipsometry signature) at the end of the first super-cycle and of 3 nm at the end of the 7th super-cycle. This thickness increase is within the measurement uncertainty (±1 nm) of our ellipsometer. It may be due to further oxidation of the silicon substrate due to diffusion.

This result shows that the as-defined Ar^+ sputtering step enables Ta_2O_5 etching with a high selectivity with respect to the SiO_2 underlayer. Figure 6 also indicates that during the 6 subsequent super-cycles, the global Ta_2O_5 thickness increase over one super-cycle drops to zero, once the 2 nm thick SiO_2 interface is formed during the first super-cycle. Indeed, the difference in the thickness increase between the first super-cycle (10 nm) and other cycles (12 nm) can be attributed to different substrate surfaces exposed to the precursor flux in the initial stages of the PEALD process. In fact, the Si substrates are known to inhibit the PEALD nucleation, as compared to oxidized substrates, which are readily reacting substrates.

Moreover, the slight rise in the ellipsometry signature that is systematically observed when the etching step is stopped is attributed to a re-deposition of etched by-products. This phenomenon is most likely to happen during the sputtering process.

These results can be taken as evidence that the thus-defined ASD process has reached a steady state regime, with the complete Ar^+ sputtering of the Ta_2O_5 material on horizontal surfaces coated during the previous PEALD step.

The topographical selectivity of the as-optimized ASD process is illustrated in Fig. 7. It shows cross-sectional SEM images

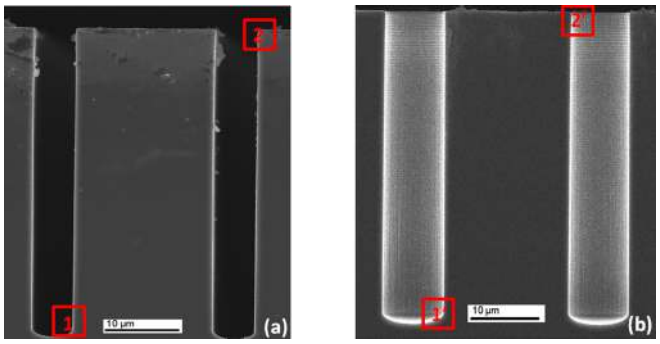

FIG. 7. SEM cross-sectional images after exposure to 7 super-cycles of the ASD process for (a) trenches and (b) holes.

of the two 3D patterned substrates with trenches [Fig. 7(a)] and holes [Fig. 7(b)] having an aspect ratio AR equal to 7 and 5, respectively.

These two images are zoomed in the bottom and top regions for both hole and trench profiles in Figs. 8 and 9, respectively. Each one of these regions is identified by a red square in Fig. 7. As expected, we observe that only vertical surfaces of both hole and trench 3D patterns are coated by Ta_2O_5 thanks to the use of the optimized ASD process. The nodules depicted on the horizontal surfaces in Fig. 9 are most likely dust particles, because the SEM tool is installed in a grey room environment. The 2 nm thick SiO_2 interface layer does not show up on these SEM pictures, due to its small relative thickness.

This selectivity is attributed to the directionality of Ar^+ sputtering ions extracted from the plasma by the dc bias voltage of −239 V. Thus, only Ta_2O_5 coated horizontal surfaces are exposed to the Ar^+ ion flux and are selectively etched away, whereas vertical sidewalls of the 3D structures remain unaffected by the introduction of this etching step every 100 standard PEALD cycles.

We have designed a topographically selective deposition process based on the alternate use of a standard PEALD deposition process and the subsequent *in situ* Ar^+ plasma anisotropic etching step. The produced anisotropic selective deposition shows up only on vertical surfaces and not on horizontal surfaces of 3D patterned structures. The results obtained in this work emphasize the importance of accurate ion energy control with substrate biasing for topographically selective deposition.

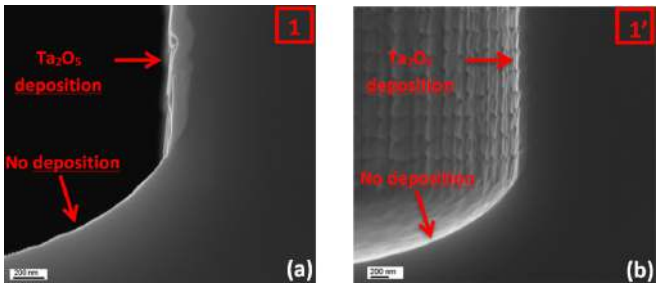

FIG. 8. SEM cross-sectional images for the trench and hole zoomed at (a) position 1 and (b) position 1′.

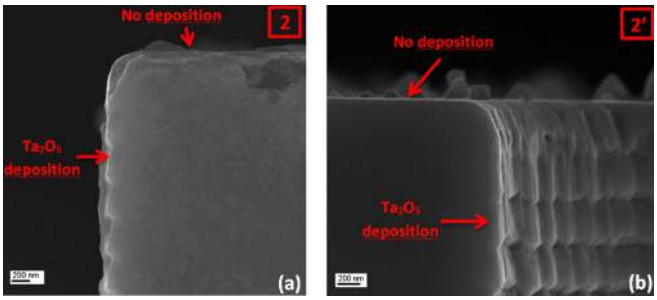

FIG. 9. SEM cross-sectional images for trenches and holes: zoom at (a) position 2 and (b) position 2′.

Thanks to its relative simplicity, this selective deposition process can potentially reduce time and costs in the fabrication of advanced integrated devices, such as 3D coaxial MIM devices with increased capacitance density or vertically coated nanopillar devices for CMOS technologies.

We acknowledge the financial support of LabEx Minos ANR-10-LABX-55-01 for Ph.D. funding of A.C. and S.B.

REFERENCES

[1]A. Raley, S. Thibaut, N. Mohanty, K. Subhadeep, S. Nakamura, A. Ko, D. OMeara, K. Tapily, S. Consiglio, and P. Biolsi, Proc. SPIE **9782**, 97820F (2016).
[2]A. J. M. Mackus, A. A. Bol, and W. M. M. Kessels, Nanoscale **6**, 10941 (2014).
[3]R. Clark, K. Tapily, K.-H. Yu, T. Hakamata, S. Consiglio, D. O'Meara, C. Wajda, J. Smith, and G. Leusink, APL Mater. **6**, 058203 (2018).
[4]K. Galatsis, K. L. Wang, M. Ozkan, C. S. Ozkan, Y. Huang, J. P. Chang, H. G. Monbouquette, Y. Chen, P. Nealey, and Y. Botros, Adv. Mater. **22**, 769 (2010).
[5]E. Farm, M. Kemell, M. Ritala, and M. Leskel, Chem. Vap. Deposition **12**, 415–417 (2006).
[6]R. Chen, H. Kim, P. C. Mclntyre, and S. F. Bent, Appl. Phys. Lett. **84**, 4017 (2004).
[7]R. Chen and S. F. Bent, Adv. Mater. **18**, 1086 (2006).
[8]F. S. M. Hashemi, C. Prasittichai, and S. F. Bent, ACS Nano **9**, 8710 (2015).
[9]A. J. M. Mackus, N. F. W. Thissen, J. J. L. Mulders, P. H. F. Trompenaars, M. A. Verheijen, A. A. Bol, and W. M. M. Kessels, J. Phys. Chem. C. **117**, 10788 (2013).
[10]K. J. Park, J. M. Doub, T. Gougousi, and G. N. Parsons, Appl. Phys. Lett. **86**, 051903 (2005).
[11]M. Yan, Y. Koide, J. R. Babcock, P. R. Markworth, J. A. Belot, T. J. Marks, and R. P. H. Chang, Appl. Phys. Lett. **79**, 1709 (2001).
[12]M. H. Park, Y. J. Jang, H. M. Sung-Suh, and M. M. Sung, Langmuir. **20**, 2257 (2004).
[13]E. Färm, M. Vehkamäki, M. Ritala, and M. Leskelä, Semicond. Sci. Technol. **27**, 074004 (2012).
[14]M. Fang and J. C. Ho, ACS Nano **9**, 8651 (2015).
[15]B. Kalanyan, P. C. Lemaire, S. E. Atanasov, M. J. Ritz, and G. N. Parsons, Chem. Mater. **28**, 117–126 (2016).
[16]A. Sinha, D. W. Hess, and C. L. Henderson, J. Electrochem. Soc. **153**, G465 (2006).
[17]S. E. Atanasov, B. Kalanyan, and G. N. Parsons, J. Vac. Sci. Technol., A **34**, 01A148 (2016).
[18]A. Haider, P. Deminskyi, T. M. Khan, H. Eren, and N. Biyikli, J. Phys. Chem. C **120**, 26393 (2016).
[19]A. Mameli, M. J. M. Merkx, B. Karasulu, F. Roozeboom, W. M. M. Kessels, and A. J. M. MacKus, ACS Nano **11**, 9303 (2017).
[20]J. A. Singh, N. F. W. Thissen, W. H. Kim, H. Johnson, W. M. M. Kessels, A. A. Bol, S. F. Bent, and A. J. M. Mackus, Chem. Mater. **30**, 663 (2018).
[21]K. J. Hughes and J. R. Engstrom, J. Vac. Sci. Technol., A **30**, 01A102 (2012).
[22]R. C. Longo, S. McDonnell, D. Dick, R. M. Wallace, Y. J. Chabal, J. H. G. Owen, J. B. Ballard, J. N. Randall, and K. Cho, J. Vac. Sci. Technol., B **32**, 03D112 (2014).
[23]D. Dick, J. B. Ballard, R. C. Longo, J. N. Randall, K. Cho, and Y. J. Chabal, J. Phys. Chem. C **120**, 24213 (2016).
[24]R. Vallat, R. Gassilloud, B. Eychenne, and C. Vallée, J. Vac. Sci. Technol., A **35**, 01B104 (2017).
[25]H. B. Profijt, S. E. Potts, M. C. M. van de Sanden, and W. M. M. Kessels, J. Vac. Sci. Technol., A **29**, 050801 (2011).
[26]H. B. Profijt, P. Kudlacek, M. C. M. van de Sanden, and W. M. M. Kessels, J. Electrochem. Soc. **158**, G88 (2011).
[27]T. Faraz, H. C. M. Knoops, M. A. Verheijen, C. A. A. van Helvoirt, S. Karwal, A. Sharma, V. Beladiya, A. Szeghalmi, D. M. Hausmann, J. Henri, M. Creatore, and W. M. M. Kessels, ACS Appl. Mater. Interfaces **10**, 13158 (2018).
[28]H. B. Profijt, M. C. M. van de Sanden, and W. M. M. Kessels, J. Vac. Sci. Technol., A **31**, 01A106 (2013).
[29]S. Karwal, M. A. Verheijen, B. L. Williams, T. Faraz, W. M. M. Kessels, and M. Creatore, J. Mater. Chem. C **6**, 3917 (2018).
[30]R. Vallat, R. Gassilloud, O. Salicio, K. El Hajjam, G. Molas, B. Pelissier, and C. Vallée, "Area selective deposition of TiO_2 by intercalation of plasma etching cycles in PEALD process: A bottom up approach for the simplification of 3D integration scheme," J. Vac. Sci. Technol., A (submitted).
[31]W. Dong, K. Zhang, Y. Zhang, T. Wei, Y. Sun, X. Chen, and N. Dai, Sci. Rep. **4**, 4458 (2014).
[32]W. H. Kim, F. S. M. Hashemi, A. J. M. Mackus, J. Singh, Y. Kim, D. B. Semple, Y. Fan, T. K. Osborn, L. Godet, and S. F. Bent, ACS Nano **10**, 4451 (2016).
[33]D. R. Cote, S. V. Nguyen, A. K. Stamper, D. S. Armbrust, D. Tobben, R. A. Conti, and G. Y. Lee, IBM J. Res. Dev. **43**, 5 (1999).
[34]Z. Liu, Y. Zhan, G. Shi, S. Moldovan, M. Gharbi, L. Song, L. Ma, W. Gao, J. Huang, R. Vajtai, F. Banhart, P. Sharma, J. Lou, and P. M. Ajayan, Nat. Commun. **3**, 879 (2012).
[35]P. Schindler, M. Logar, J. Provine, and F. B. Prinz, Langmuir **31**, 5057 (2015).